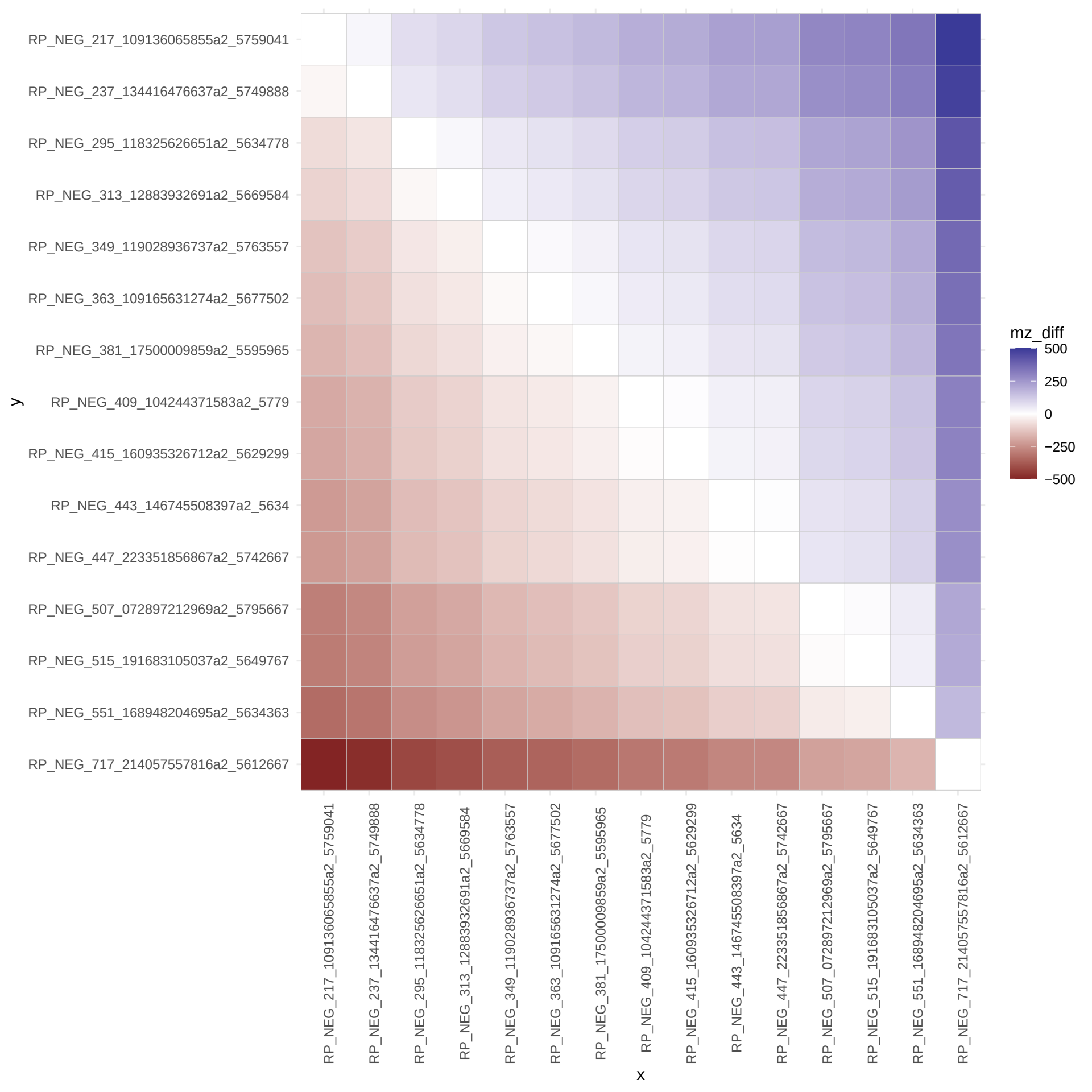
RP_NEG_217_109136065855a2_5759041
RP_NEG_237_134416476637a2_5749888
RP_NEG_295_118325626651a2_5634778
RP_NEG_313_12883932691a2_5669584
RP_NEG_349_119028936737a2_5763557
RP_NEG_363_109165631274a2_5677502
RP_NEG_381_17500009859a2_5595965
RP_NEG_409_104244371583a2_5779
RP_NEG_415_160935326712a2_5629299
RP_NEG_443_146745508397a2_5634
RP_NEG_447_223351856867a2_5742667
RP_NEG_507_072897212969a2_5795667
RP_NEG_515_191683105037a2_5649767
RP_NEG_551_168948204695a2_5634363
RP_NEG_717_214057557816a2_5612667
y
x
mz_diff
500
250
0
−250
−500

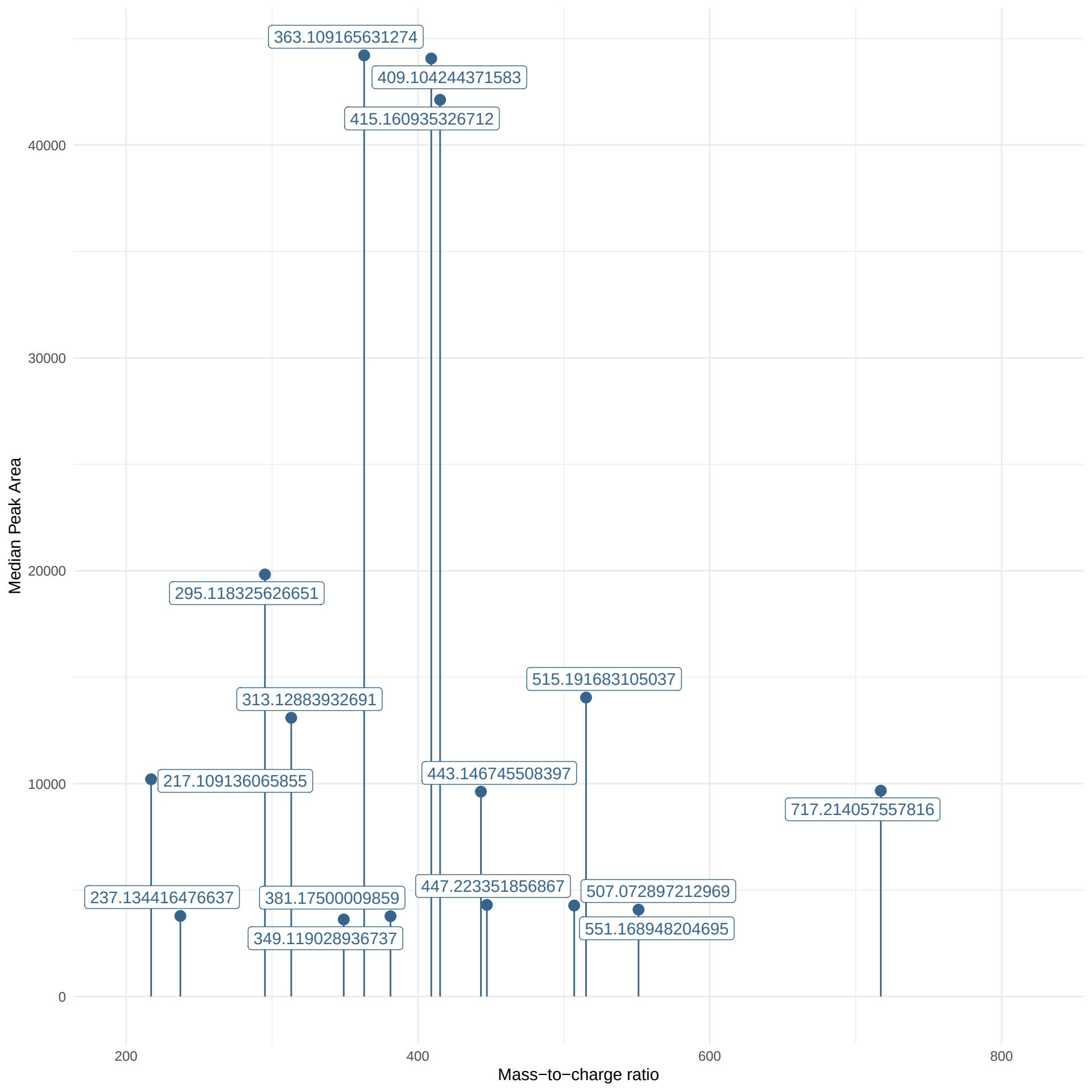
363.109165631274
409.104244371583
415.160935326712
295.118325626651
313.12883932691
217.109136065855
515.191683105037
443.146745508397
717.214057557816
237.134416476637
381.17500009859
447.223351856867
507.072897212969
551.168948204695
349.119028936737
40000
30000
20000
10000
0
Median Peak Area
200
400
600
800
Mass−to−charge ratio

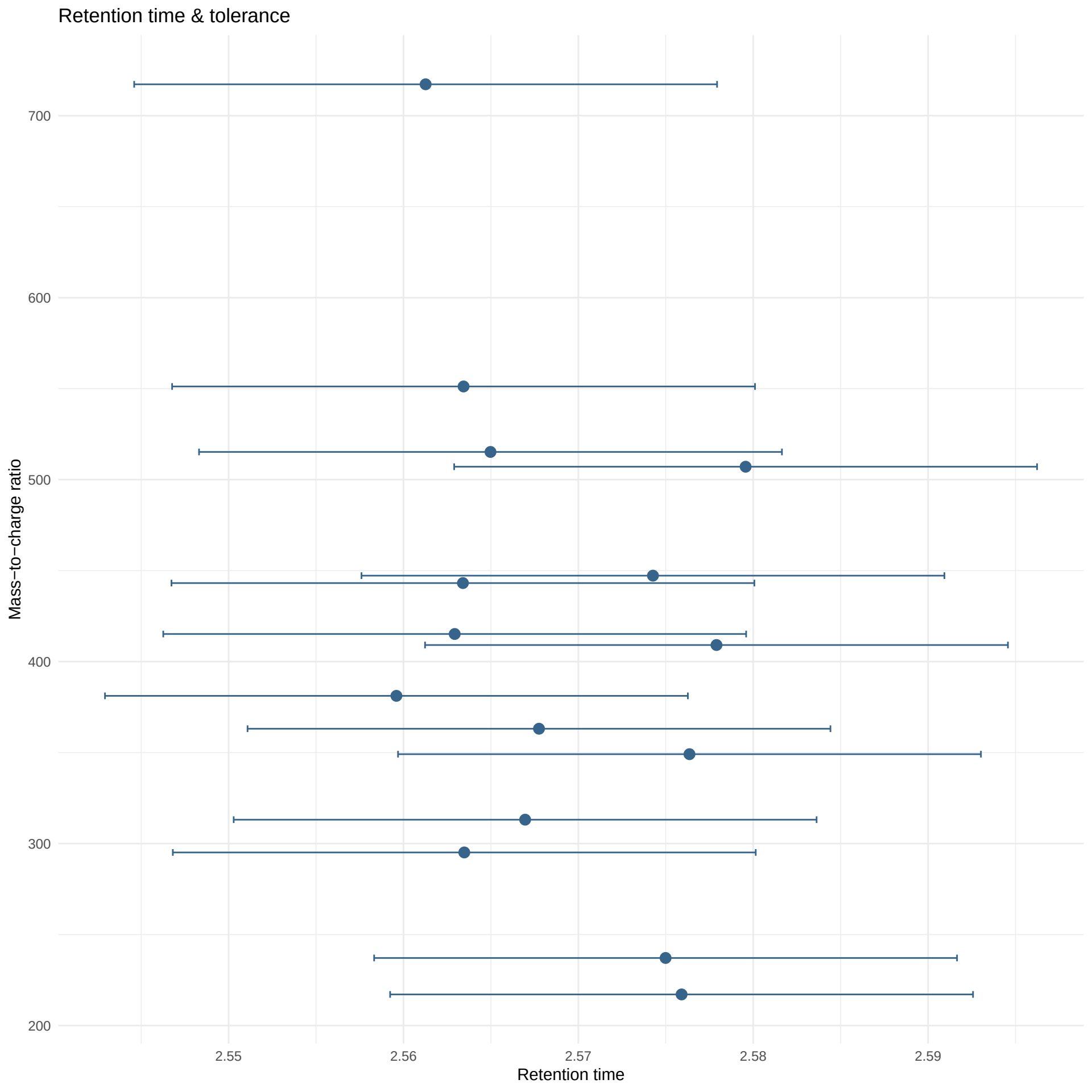
Retention time & tolerance
Mass−to−charge ratio
700
600
500
400
300
200
2.55
2.56
2.57
2.58
2.59
Retention time

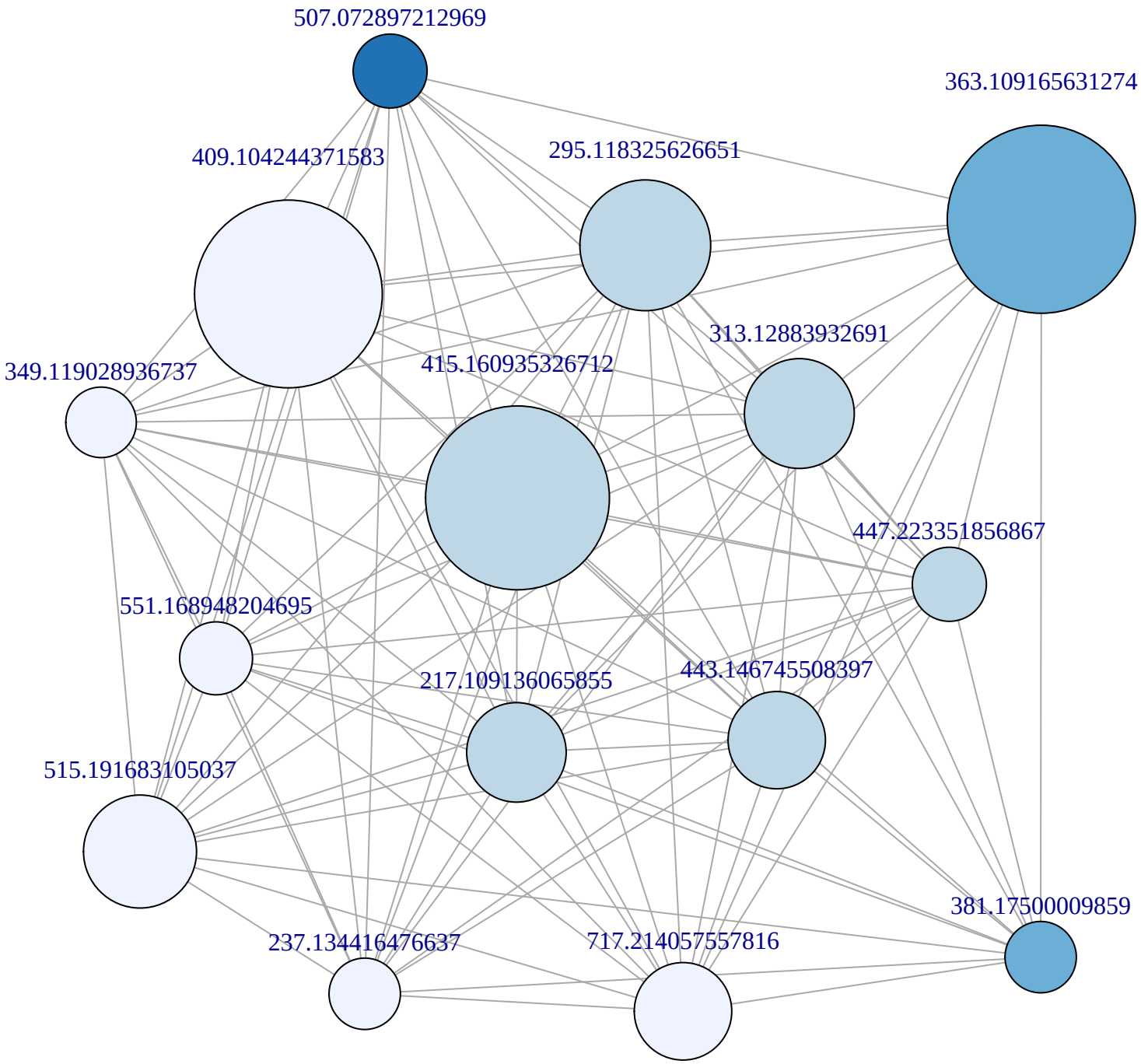
507.072897212969
363.109165631274
409.104244371583
295.118325626651
313.12883932691
349.119028936737
415.160935326712
447.223351856867
551.168948204695
217.109136065855
443.146745508397
515.191683105037
381.17500009859
237.134416476637
717.214057557816